Med Chem Res (2011) 20:321–332
DOI 10.1007/s00044-010-9323-4

MEDICINAL CHEMISTRY RESEARCH

ORIGINAL RESEARCH

Molecular modeling studies, synthesis and biological evaluation of derivatives of *N*-phenylbenzamide as *Plasmodium falciparum dihydroorotate dehydrogenase* (*Pf*DHODH) inhibitors

Kumar R. Desai · Mushtaque S. Shaikh · Evans C. Coutinho

Received: 5 June 2009 / Accepted: 12 February 2010 / Published online: 4 March 2010

Abstract The search for new antimalarial agents is necessary as current drugs in the market have become vulnerable due to the emergence of resistant strains of *Plasmodium falciparum* (*Pf*). The enzyme *dihydroorotate dehydrogenase* (*Pf*DHODH) is a validated target for development of antimalarial agents. *Pf*DHODH is a crucial enzyme in the de novo pyrimidine biosynthesis pathway and is essential for the growth of the parasite. In this article, we report the design, synthesis and evaluation of benzanilides as inhibitors of *Pf*DHODH. From the pool of molecules designed using molecular modeling techniques, candidates were shortlisted for further evaluation based on docking scores and 3D-QSAR studies. The activities of these shortlisted analogs were predicted from CoMFA and CoMSIA models. The most promising molecules were synthesized using solvent-free microwave-assisted synthesis and their structures characterized by spectroscopic techniques. The molecules were screened for in vitro antimalarial activity by the whole cell assay method. Two molecules viz. KMC-3 and KMC-15 were found to be active at 8.7 and 5.7 μM concentrations, respectively.

Keywords *Pf*DHODH · Antimalarials · *N*-Phenylbenzamide · Docking · 3D-QSAR

Electronic supplementary material The online version of this article (doi:10.1007/s00044-010-9323-4) contains supplementary material, which is available to authorized users.

K. R. Desai · M. S. Shaikh · E. C. Coutinho (✉)
Department of Pharmaceutical Chemistry, Bombay College of Pharmacy, Kalina, Santacruz (E), Mumbai 400 098, India
e-mail: evans@bcpindia.org

Introduction

Malaria is a devastating infectious disease affecting a significant portion of the world's population; approximately 41% reside in locations where this disease is transmitted. The Centre for Disease Control estimated that 0.7–2.7 million people die annually from this disease (Centre for Disease Control 2005). A major contributor to malarial morbidity and mortality is almost certainly the increasing resistance of malaria parasites to current therapy (Ridley 2002).

Current antimalarial drug therapy focuses on three families of compounds—the quinolines (quinine, chloroquine, amodiaquine, mefloquine), the antifolates (sulphadoxine-pyrimethamine) and the artemisinin derivatives (artemether, arteether, artesunate). All of them have great clinical significance but possess liabilities related to resistance, compliance, safety, cost and/or ineffectiveness (Chiang *et al*., 2006, Freundlich *et al*., 2006). To avoid an ever increasing toll of malaria globally, especially in India and other tropical countries, it is imperative to rapidly put into action a strategic plan for the discovery and development of novel antimalarial compounds that are not encumbered by existing mechanisms of drug resistance and related problems. More recently, an improved understanding of the biochemistry of malarial parasites has identified many potential targets for new drugs and helped shed light on the mode(s) of action of older drugs (Becker and Kirk 2004). An ideal target for chemotherapy is one which is not common to the malarial parasite and humans since it would impart a clear selectivity for new drugs. Unfortunately, it may not always be possible to explore or exploit unique targets. In many cases, one has to focus on non-selective targets. In such instances, there is significant scope for development of drugs if structural differences

between the targets could be exploited (Breman, 2001). The enzyme *dihydroorotate dehydrogenase* (DHODH) of *Plasmodium* is one such target suitable for design and discovery of novel therapeutics.

P. falciparum dihydroorotate dehydrogenase (*Pf*DHODH)

Dihydroorotate dehydrogenase (DHODH), located in the outer membrane of the mitochondria, is a crucial enzyme in the de novo pyrimidine biosynthesis pathway. It catalyses the fourth step in the pathway which is the reduction of dihydroorotate to orotate with flavin nucleotide as the cofactor. The biosynthetic pathway is depicted in Fig. 1.

DHODH is essential for parasite growth and has been validated as an antimalarial drug target. An RNA interference (RNAi) study of *Plasmodium falciparum* DHODH (*Pf*DHODH; EC: 1.3.99.11, 1.3.3.1) indicated a good correlation between decreased levels of DHODH *m*RNA and parasitic growth (McRobert and McConkey 2002). Hence, *Pf*DHODH can be exploited as a novel drug target for development of new antimalarial agents (Heikkila *et al.*, 2007). Several derivatives of triazolopyrimidine (Phillips *et al.*, 2008; Gujjar *et al.*, 2009), benzanilide (Baldwin *et al.*, 2005; Heikkila *et al.*, 2006), naphthamide and urea (Baldwin *et al.*, 2005) have been reported to inhibit *Pf*DHODH. Yet, there is a good scope for design and/or optimization of these molecules owing to either (a) their toxic nature, e.g. Leflunomide (Arava or A771726) which causes several untoward effects (Davis *et al.*, 1996; Hamilton *et al.*, 1999; Li and Lin 2002; Elkayam *et al.*, 2003; Kobayashi *et al.*, 2004; Yao *et al.*, 2004a, b; Zhang *et al.*, 2005; Otsuka *et al.*, 2008; Zhang *et al.*, 2008; Baumann *et al.*, 2009) or (b) poor activity, e.g. brequinar (Boa *et al.*, 2005). In this article, we report our attempts to design some new *Pf*DHODH inhibitors using molecular modeling techniques.

Materials and methods

Computational details

The computational studies were carried on a PC with an AMD 3.0-GHz processor and 1.5-GB RAM operating under the RedHat Linux Enterprise WS4 OS. Molecules were built and their geometries optimized with the suite of programs in *Sybyl* (*v7.1,* Tripos Inc., St. Louis, Missouri, USA). The 3D-QSAR techniques of Comparative Molecular Field Analysis (CoMFA, Cramer *et al.*, 1988, 1989) and Comparative Molecular Similarity Indices Analysis (CoMSIA, Klebe *et al.*, 1994, 1998) were carried out with *Sybyl* (v*7.1*). The molecular docking studies were carried out using the software *GOLD v*3.0.1 (CCDC, Cambridge, UK).

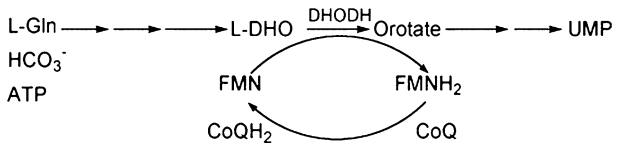

Fig. 1 De novo pyrimidine biosynthesis pathway

Docking studies

Molecular docking has been utilized to understand the conformation and configuration of the ligands that bind to *Pf*DHODH. This also provided a framework for receptor-based alignment of the ligands which was used as input for the 3D-QSAR studies.

Ligand preparation

Inhibitors of *Pf*DHODH were built using molecule **22** (Table 1), popularly known as A771726 [2-cyano-3-hydroxy-(4-trifluoromethylphenyl)-*n*-butyramide]. A771726, the co-crystallized ligand in the crystal structure of *Pf*DHODH with PDB code 1TV5 (Hurt *et al.*, 2006), was extracted and used as the template for building other molecules with the *Builder* module in *Sybyl*. The geometries of analogs of *N*-phenylbenzamide, *N*-phenylarylamides, *N*-arylbenzamides and *N,N′*-diaryl urea (Tables 1, 2, S1 of supplementary data) were optimized by energy minimization using the conjugate gradient method with the Tripos force field and Gasteiger Hückel charges for all atoms, until a gradient of 0.01 kcal/mol/Å was reached. The dielectric constant was set to 1.0.

Protein preparation

The crystal structure of *Pf*DHODH with PDB code 1TV5 was used for the docking studies. The enzyme exists as a tetramer in the crystal. The actual docking studies were done with the monomeric unit of the enzyme, as the active site resides deep within the enzyme. The water molecules in the crystal were not considered during docking. The ligand and the cofactor were deleted from the protein ligand complex; this was followed by 'cleaning up' the protein structure, addition of hydrogens to all heavy atoms and the assignment of Gasteiger Hückel charges to the atoms of the protein using the *Biopolymer* module in *Sybyl*. For compatibility with the GOLD program, *Sybyl* atom and bond types were assigned to the protein atoms. The side chains of aspartate, glutamate, lysine and arginine residues were kept in their ionized state corresponding to pH 8.5,

Table 1 List of inhibitors known to be active against *Pf* DHODH

Sr. No.	Compounds	IC_{50} (HTS)	pIC_{50}
1	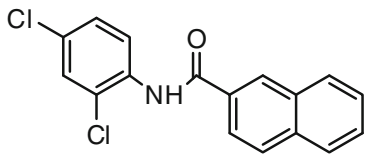	0.10	7.00
2	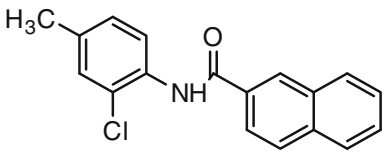	0.15	6.82
3	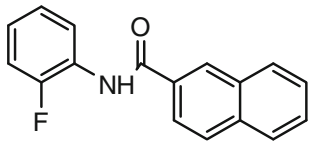	0.25	6.60
4	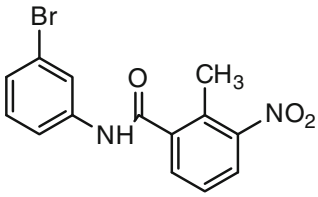	0.10	7.00
5	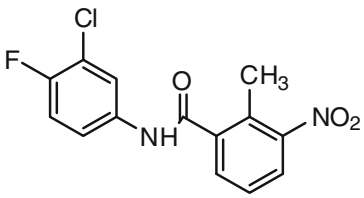	0.10	7.00
6	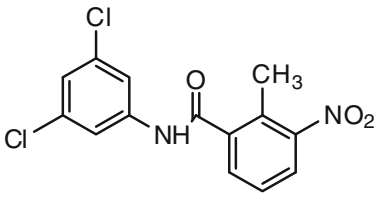	0.15	6.82

Table 1 continued

Sr. No.	Compounds	IC_{50} (HTS)	pIC_{50}
7	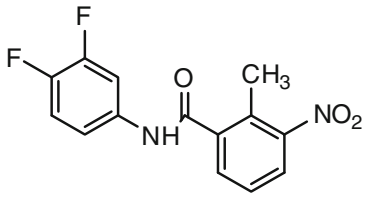	0.15	6.82
8	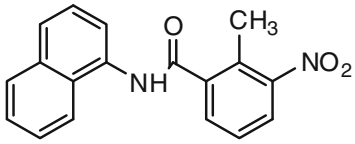	0.10	7.00
9	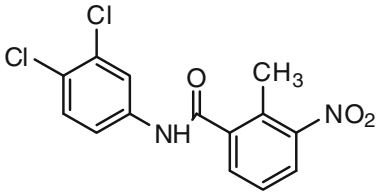	0.25_3	6.60
10	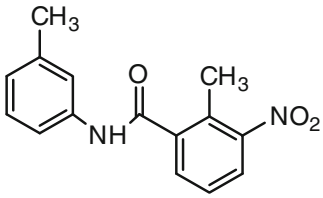	0.30_3	6.52
11	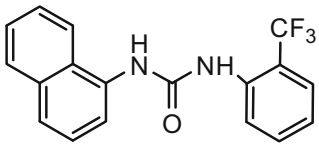	0.20	6.70
12	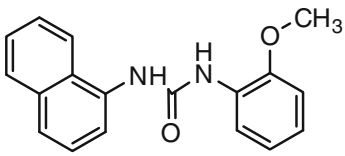	0.25	6.60

Table 1 continued

Sr. No.	Compounds	IC_{50} (HTS)	pIC_{50}
13	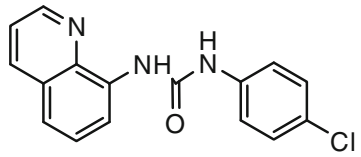	0.55	6.26
14	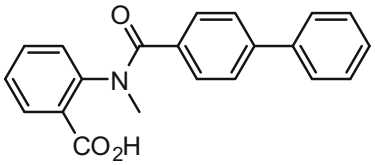	42.6	4.37
15	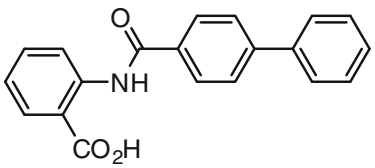	153.5	3.81
16	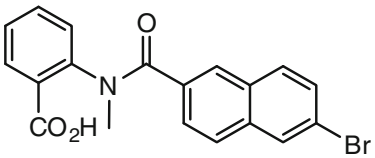	93.4	4.03
17	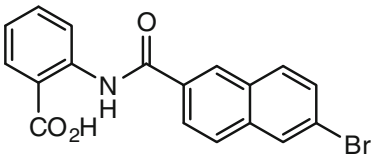	142.6	3.85
18	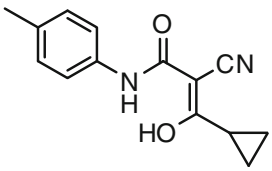	880	3.06

Table 1 continued

Sr. No.	Compounds	IC_{50} (HTS)	pIC_{50}
19	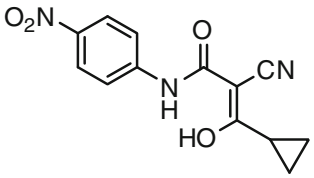	543	3.27
20	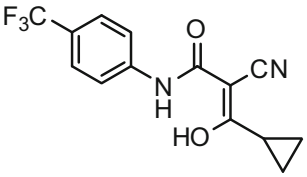	1080	2.97
21	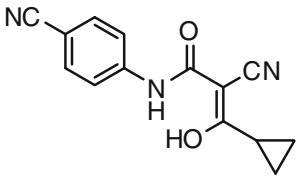	712	3.15
22	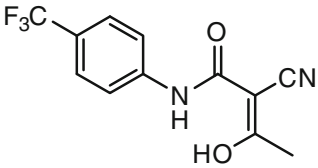	190.1	3.72

while histidine was unprotonated (corresponding to the δ tautomer) at this pH.

Docking protocol

With any docking program, it is important to determine the effectiveness of the algorithm for the protein under study (*validation*). Validation of the docking protocol was judged from the superposition of conformations obtained by docking and the native structure of the ligand A771726 in the PDB structure (PDB code: 1TV5). The docking study was carried out using *GOLD v*3.1 (CCDC Ltd., Cambridge, UK) in conjunction with *Sybyl v7.1* (Tripos Inc., St. Louis,

Table 2 Structures of the *N*-phenylbenzamide derivatives designed and synthesized as *Pf*DHODH inhibitors

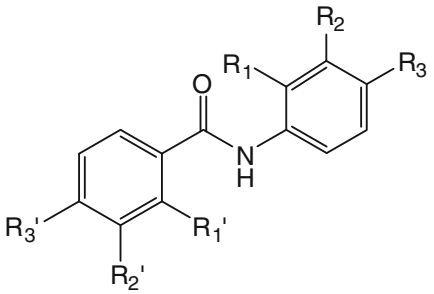

Compounds	R_1	R_2	R_3	R_1'	R_2'	R_3'
KMC-1	–H	–H	–H	–H	–H	–H
KMC-2	–Cl	–H	–H	–H	–H	–H
KMC-3	–H	–Cl	–H	–H	–H	–H
KMC-4	–H	–H	–Cl	–H	–H	–H
KMC-5	–Cl	–Cl	–H	–H	–H	–H
KMC-6	–Cl	–H	–Cl	–H	–H	–H
KMC-7	$–NO_2$	–H	–H	–H	–H	–H
KMC-8	–H	$–NO_2$	–H	–H	–H	–H
KMC-9	–H	–H	$–NO_2$	–H	–H	–H
KMC-10	$–CH_3$	–H	–H	–H	–H	–H
KMC-11	–H	$–CH_3$	–H	–H	–H	–H
KMC-12	–H	–H	$–CH_3$	–H	–H	–H
KMC-13	–H	–Cl	$–OCH_3$	–H	–H	–H
KMC-14	–H	–H	–Br	–H	–H	–H
KMC-15	–H	–Cl	–F	–H	–H	–H

Missouri, USA) with which it shares atom and bond types. GOLD is a genetic algorithm for docking flexible ligands into protein binding sites. The configuration of A771726 in the crystal structure of *P. falciparum* DHODH (PDB code: 1TV5) was used for an initial alignment of other ligands in the active site of the enzyme which was defined by residues enclosed within a 6.0-Å radius from the centroid of A771726. The residues which define the active site were Tyr168, Phe171, Leu172, Cys175, Leu176, Gly181, Glu182, Cys184, His185, Phe188, Phe227, Ile263, Arg265, Ile272, Tyr528, Leu531, Val532, Gly535 and Met536. The parameters in GOLD, modified/optimized for the docking studies were (a) the dihedral angles of the ligand, (b) the ligand ring geometries (flipping ring corners), (c) the dihedral angles of protein OH and NH_3^+ groups and (d) mappings of the H-bond fitting points. At the start of a docking run, all these variables were randomized. The docking was carried for 20 Genetic Algorithm (GA) runs, which was optimum to reproduce the crystal structure. Most of the other GA parameters like the population size and the genetic operators were left at their default values.

3D-QSAR studies

We have used CoMFA and CoMSIA in order to understand the structure activity relationship and to predict the inhibitory activities and also to fine tune the structures of the *N*-phenylbenzamide analogs so as to improve their activity.

Formation of the training and test sets

The P*f*DHODH inhibitors used in the 3D-QSAR study were taken from a series of papers (Baldwin *et al.*, 2002, 2005; Heikkila *et al.*, 2006, 2007). Based on quality of the data and uniqueness of structures, 22 molecules (Table 1) shaped the dataset for the 3D-QSAR study. The training set consisted of 15 molecules, while the test set consisted of 7 molecules.

CoMFA and CoMSIA studies

Comparative molecular field analysis (CoMFA) and comparative molecular similarity indices analysis (CoMSIA) studies were carried out with the default settings for the 3D cubic lattice, the grid spacing, the probe atom and the cut-off for the interaction energy. For CoMSIA, four

Table 3 Statistical analyses of the 3D QSAR models

PLS statistics	CoMFA	CoMSIA			
Models Fields in models	Model 1 SE	Model 2 SDA	Model 3 SEA	Model 4 SEH	Model 5 EHD
n	15	15	15	15	15
r^2	0.99	0.965	0.958	0.954	0.943
q^2 (LOO)	0.62	0.79	0.64	0.63	0.74
q^2 (LGO)	0.65	0.72	0.71	0.66	0.74
$r^2_{bootstrap}$	0.99	0.99	0.99	0.99	0.99
r^2_{pred}	0.44	0.75	0.64	0.76	0.74
F	314.98	101.502	83.676	75.201	98.513
SE	0.17	0.34	0.38	0.40	0.42
PLS components	4	3	3	3	2
Field contributions					
Steric	0.384	0.065	0.07	0.076	–
Electrostatic	0.617	–	0.464	0.513	0.263
Hydrophobic	–	–	–	0.411	0.38
H-donor	–	0.492	–	–	0.357
H-acceptor	–	0.443	0.466	–	–

Fields referred: *S* steric, *E* electrostatic, *H* hydrophobic, *A* H-acceptor, *D* H-donor fields

n number of molecules, *N* optimum number of components, q^2 or r^2_{cv} cross-validated regression coefficient, r^2 noncross-validated regression coefficient, *SE* standard error of estimate, r^2_{pred} predictive (test molecules) regression coefficient, $r^2_{bootstrap}$ regression coefficient after 100 runs of bootstrap analysis, *PLS* partial least square, *LOO* leave-one-out, *LGO* leave-group-out

physicochemical properties (steric, electrostatic, hydrophobic and hydrogen bond) were explored, and the attenuation factor was set to the default value of 0.3. The CoMFA and CoMSIA descriptors were used as independent variables and the pIC_{50} values as the dependent variable in a partial least squares (PLS) regression analysis (Wold *et al.*, 1993) to derive 3D-QSAR models. The models were internally evaluated by leave-one-out (LOO) cross-validation (Richard *et al.*, 1988). The optimum number of components was determined by the SAMPLS method (Bush and Nachbar 1993) and this was subsequently used to derive the final QSAR models. In addition to the cross-validated regression coefficient q^2, the conventional regression coefficient r^2, the standard error (SE) and the F value were also computed. The models generated were also validated through calculation of r^2_{pred} of the external test set (Gramatica 2007). The robustness of the models was gauged by cross validation using leave-group-out (LGO) of 10 groups and bootstrapping (Shao 1996) carried out with 100 runs (Table 3). Other relevant data pertaining to training and test sets are given in Table 4. The CoMFA and CoMSIA models were used to predict the activities of the newly designed molecules (Table 5).

Chemical synthesis

All solvents and reagents for synthesis were of general reagent (GR) grade. All reactions were monitored by thin layer chromatography (TLC) using Merck pre-coated silica plates (GF_{254}) for completion and for establishing their purity. Melting points were recorded in open capillaries on an electrically heated melting point apparatus and are uncorrected and boiling points were recorded in a Thiele's tube. Infrared spectra were recorded (KBr disc) on a Jasco FT-IR 5300 spectrophotometer. Typically 16 scans were used with a gain of 2. ^{1}H-NMR spectra were recorded on Bruker AN500 instrument. Chemical shifts are reported in parts per million (ppm) down field from tetramethylsilane (TMS) as the internal standard and DMSO as solvent.

Synthesis of substituted N-phenylbenzamide analogs

Potassium *tert*-butoxide (1 mol) was added to a mixture of substituted aniline (1 mol) and methyl benzoate (1 mol) in a glass tube. This was inserted in a silica bath and placed inside an unmodified household microwave oven and irradiated for a specific time (Table S2 of Supplementary

Table. 4 The experimental and predicted pIC_{50} values for the training and test set molecules

Molecules	Experimental pIC_{50}	CoMFA predicted pIC_{50} (residuals)	CoMSIA predicted pIC_{50} (residuals)			
		Model 1	Model 2	Model 3	Model 4	Model 5
Training set						
3	6.6	6.46(0.14)	6.1 (0.5)	6.33(0.27)	5.96(0.64)	5.56(1.04)
6	7	6.95(0.05)	6.84(0.16)	6.8(0.2)	6.99(0.01)	6.86(0.14)
7	6.82	7.05(−0.23)	6.75(0.07)	6.97(−0.15)	7.23(−0.41)	7.16(−0.34)
8	6.82	6.49(0.33)	6.8(0.02)	6.53(0.29)	6.59(0.23)	6.8(0.02)
9	7	7.08(−0.08)	7.02(−0.02)	7.02(−0.02)	7.08(−0.08)	6.94(0.06)
10	6.52	6.58(−0.06)	6.53(−0.01)	6.56(−0.04)	6.28(0.24)	6.47(0.05)
11	6.7	6.58(0.12)	6.82(−0.12)	6.62(0.08)	6.85(−0.15)	6.89(−0.19)
13	6.26	6.41(−0.15)	6.55(−0.29)	6.4(−0.14)	6.2(0.06)	6.48(−0.22)
14	4.37	4.36(0.01)	4.35(0.02)	4.51(−0.14)	4.22(0.15)	4.23(0.14)
15	3.81	3.94(−0.13)	3.99(−0.18)	3.93(−0.12)	3.78(0.03)	3.71(0.1)
16	4.03	4.15(−0.12)	4.25(−0.22)	4.21(−0.18)	4.46(−0.43)	4.28(−0.25)
18	3.06	3.12(−0.06)	3.54(−0.48)	3.9(−0.84)	3.9(−0.84)	3.76(−0.7)
19	3.27	3.1(0.17)	2.77(0.5)	2.53(0.74)	3.03(0.24)	2.9(0.37)
21	3.15	3.17(−0.02)	3.55(−0.4)	3.08(0.07)	2.96(0.19)	3.48(−0.33)
22	3.72	3.67(0.05)	3.28(0.44)	3.73(−0.01)	3.59(0.13)	3.61(0.11)
Test set						
1	7	6.067(0.933)	6.053(−5.12)	6.176(−11.296)	5.856(−17.152)	5.557(−22.709)
2	6.82	6.09(0.73)	6.116(5.386)	6.141(−11.527)	5.811(−17.338)	5.553(−22.891)
5	7	6.115(0.885)	6.899(6.014)	6.737(−12.751)	6.835(−19.586)	6.998(−26.584)
9	6.6	6.019(0.581)	6.449(−5.868)	6.574(−12.442)	6.122(−18.564)	6.293(−24.857)
12	6.6	6.413(0.187)	6.406(−6.219)	6.001(−12.22)	6.139(−18.359)	6.579(−24.938)
17	3.85	6.625(−2.775)	5.615(−8.39)	6.111(−14.501)	5.108(−19.609)	4.807(−24.416)
20	2.97	2.279(0.691)	3.518(−2.827)	3.421(−6.248)	3.394(−9.642)	3.5(−13.142)

Table. 5 Prediction of the activity of the newly designed P*f* DHODH inhibitors based on the CoMFA and CoMSIA models

Molecules	Predicted pIC_{50} based on CoMFA	Predicted pIC_{50} based on CoMSIA			
Models:	Model 1	Model 2	Model 3	Model 4	Model 5
KMC-1	6.44	4.84	5.67	5.34	4.67
KMC-2	6.50	4.87	5.73	5.41	4.68
KMC-3	5.96	4.79	5.56	5.25	4.65
KMC-4	4.65	5.16	5.63	4.82	4.59
KMC-5	6.00	5.04	5.58	5.23	4.78
KMC-6	5.30	5.53	5.88	5.58	5.32
KMC-7	6.24	4.73	5.48	5.49	4.51
KMC-8	5.88	4.76	5.43	4.95	4.25
KMC-9	5.28	5.30	5.33	4.96	4.97
KMC-10	6.12	4.88	5.73	5.39	4.72
KMC-11	5.93	4.86	5.57	5.24	4.67
KMC-12	4.65	5.12	5.55	4.73	4.50
KMC-13	5.70	5.12	5.73	5.30	5.00
KMC-14	4.73	5.12	5.61	4.79	4.58
KMC-15	5.36	4.95	5.10	4.86	4.36

data) at its full power of 850 W. On completion of the reaction, as determined by TLC (hexane: EtOAc, 4:1 v/v), the reaction mixture was extracted into ethyl acetate (Perreux *et al.*, 2003, Otsuka *et al.*, 2008). The extracts were dried over anhydrous sodium sulphate and the solvent removed under reduced pressure to afford a residue that upon trituration with *n*-hexane gave a pure product.

Evaluation of antimalarial activity

The antimalarial activity was evaluated against two strains of *P. falciparum* viz. NF54 and K1 by the *^{3}H-hypoxanthine uptake method* (Quashie, *et al.*, 2006). The NF54 strain is sensitive to all drugs, while the K1 strain is resistant to chloroquine and pyrimethamine. An in vitro assay involving incorporation of ^{3}H-hypoxanthine was carried out in a Coaster™ 96-well microtiter plate system and the tests were also carried out for six drugs in duplicates. The drugs, chloroquine diphosphate (Sigma C6628), artemisinin (Sigma 36159-3), artesunate (Mepha), OZ 277 (Vennerstorm lab), atovaquone (GSK) and proguanil (Roche) were the reference standards.

Stock solutions of the drugs were made in DMSO and for assay a four times dilute solution was used. The screening medium consisted of RPMI (10.44 g/l) supplemented with HEPES (5.94 g/l), $NaHCO_3$, (2.1 g/l), Neomycine (100 µg/ml) and Albumax® II (5.0 g/l). The hypoxanthine solution was made by double dilution of a 5.0 mCi/5.0 ml solution in 50% ethanol. 1.0 ml of this solution was diluted 50 times with screening medium.

For evaluation of antimalarial activity, the parasites/cells were cultured in different concentration of test compounds in media containing reduced concentration of hypoxanthine, after which ^{3}H hypoxanthine was added for an additional incubation period before the cells were harvested and the radioactivity measured. The percent reduction in ^{3}H hypoxanthine uptake by the molecules was calculated by the formula:

$$\%\ \text{Reduction in } {}^3\text{H hypoxantine uptake} = \frac{100 \times \text{geometric mean cpm of no drug sample} - \text{mean cpm of test samples}}{\text{Geometric mean cpm of no drug sample}}$$

where cpm is counts per minute.

Percent reductions were used to plot percentage inhibition of growth as a function of drug concentration. The IC_{50} values were determined by linear regression analyses on the linear segments of the dose

response curve (Fidock *et al.*, 2004, Kalra *et al.*, 2006).

Results and discussion

Docking studies

Docking studies of the *N*-arylbenzamide have been reported by Heikkila *et al*. (2006); in addition, the authors have discussed the design and synthesis of *N*-(2-carboxylic acid)phenylarylamides (Heikkila *et al.*, 2006). While using this work as a base, we have tried to improve on the design by studying the effects of many other substitutions on the efficacy and binding affinity of the inhibitors to *Pf*DHODH. The docking studies were used to determine the binding orientation of some of the known as well as the new ligands designed by us. The set of known molecules comprised aromatic amides and urea derivatives. In the docking studies, it was evident that some of the molecules could adopt different orientations in the active site and this suggested that there exists a good scope for the design of inhibitors of varying structures.

The docking studies were carried out with the X-ray crystallographic structure of *Pf*DHODH co-crystallized with the inhibitor A771726. Validation of the docking strategy was done by running the protocol for known ligands and seeing if the protocol could reproduce their crystal poses. It was found that most of the known ligands docked in the expected mode except for some where a switch in the orientation of the 2-cyano and the 3-hydroxy functionalities was seen, for e.g. A771726 (Fig. 2).

Using several combinations of aromatic acids/ester and amines, a virtual library of molecules was prepared. This library consists of derivatives of *N*-phenylbenzamide with various substitutions on both aromatic rings (Tables 2, S1A in Supplementary data) and (*N*-aryl)arylamides with a variety of aryl rings (Table S1B in Supplementary data). Thus, an extensive library of almost 80 molecules was generated. The molecules in this library were docked using the program *GOLD*. Based on the docking results (Table S3 in supplementary data), *N*-phenylbenzamide analogs were taken up for further studies. Out of several *N*-phenylbenzamide analogs designed by us, 15 molecules (Table 2) were selected for synthesis and biological evaluation, based on their docking scores, binding interactions with the residues in the active site and their activities predicted by the CoMFA and CoMSIA models.

New findings from docking studies

Some of the newly designed molecules were seen to be involved in similar interactions with the enzyme like A771726 in its crystal. These are hydrogen bond interactions with the residues Arg265, His182 and Tyr528 (Fig. 3). The docking scores of some of the designed molecules were comparable with the reference ligand (A771726). Of the two isomers of *N*-naphthylbenzamide, β-naphthylbenzamide had a lower docking score when compared to the α-isomer. The urea derivatives were also found to dock nicely into the active site and results for *N,N′*-diarylureas will be published elsewhere.

With respect to *N*-phenylbenzamides, it was observed that the receptor has a very small pocket around ring A

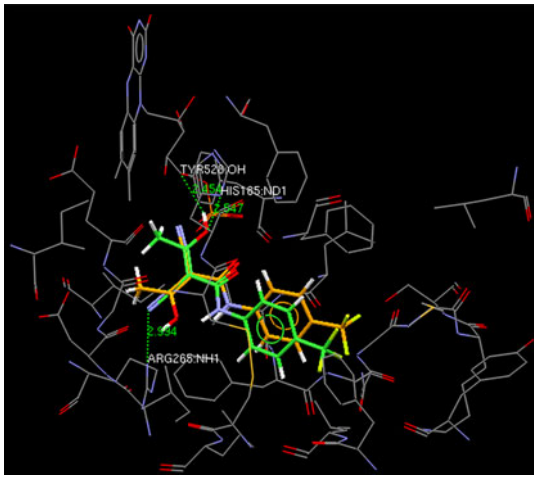

Fig. 2 Validation of the docking strategy using GOLD. Structure shown in *yellow* represents pose of A771726 as seen in the crystal, while the pose of A771726 obtained by docking with GOLD is shown in *green*. (Color figure online)

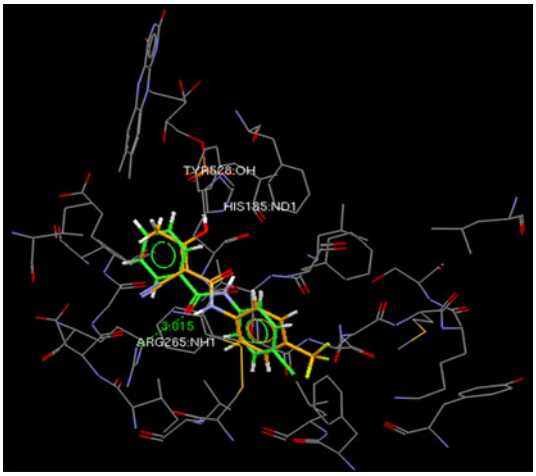

Fig. 3 The pose of *N*-(4-chlorophenyl)benzamide shown in *green* colour obtained by docking with GOLD. The residue ARG265 can be seen in an H-bonding with the carbonyl of the ligand. Note that the binding can be enhanced by adding substituents on both the aromatic rings. (Color figure online)

(Fig. 4), being able to accommodate only small size substituents on ring A. However, there is a large space around ring B that makes room for bulky groups on ring B. With this revelation, the *N*-phenylbenzamide derivatives listed in Table 2 have been designed.

3D-QSAR and prediction of activity

Various CoMFA and CoMSIA models were generated based on receptor-based alignment of the molecules. All five models (one CoMFA and four CoMSIA) were selected from the 80 odd models that were generated; the selection being guided by statistical characteristics.

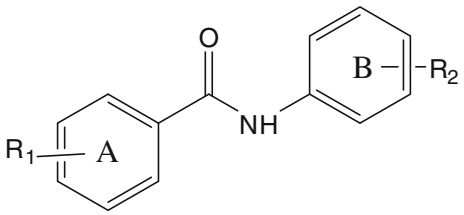

Fig. 4 Labels for the two aromatic rings in *N*-phenylbenzamide derivatives

The CoMFA electrostatic contours shown in Fig. 5a indicate that activity can be improved by introduction of electronegative atoms at the *ortho*-positions of ring B and at the *meta*-/*para*-regions of ring A (red contour). Similarly, the *ortho* region in ring A and *para*-position in ring B are surrounded by blue contours depicting a need for electropositive groups. The steric contours (Fig. 5b) suggest that the space around ring A could bear bulk more so at the *ortho*- than the *meta*-position. A strong disfavour for bulky substitutions was seen in the *para*-position of ring A. The ring B can bear a little bulk at its *meta*-position but not in the *para*-region. These facts support the better binding of the N-α-naphthyl analogs over other derivatives.

In the CoMSIA studies, almost 30 different models were derived using different combination of fields (steric, electrostatic, hydrophobic, hydrogen bond donor and hydrogen bond acceptor which are indicated by the letters S, E, H, D and A respectively) and using activity data from HTS assay.

The hydrophobic contours have been explained based on model 3 (SHE fields) and model 5 (EDH fields), while the H-bond acceptor and donor contours have been explained based on model 2 (SDA fields). The hydrophobic contours (Fig. 6a) are observed to follow an interesting pattern

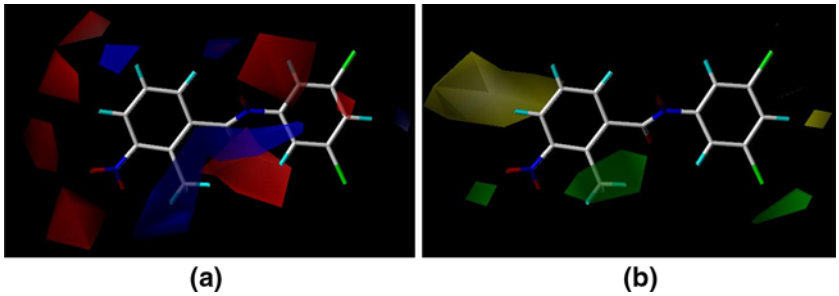

Fig. 5 CoMFA contour maps **a** electrostatic **b** steric

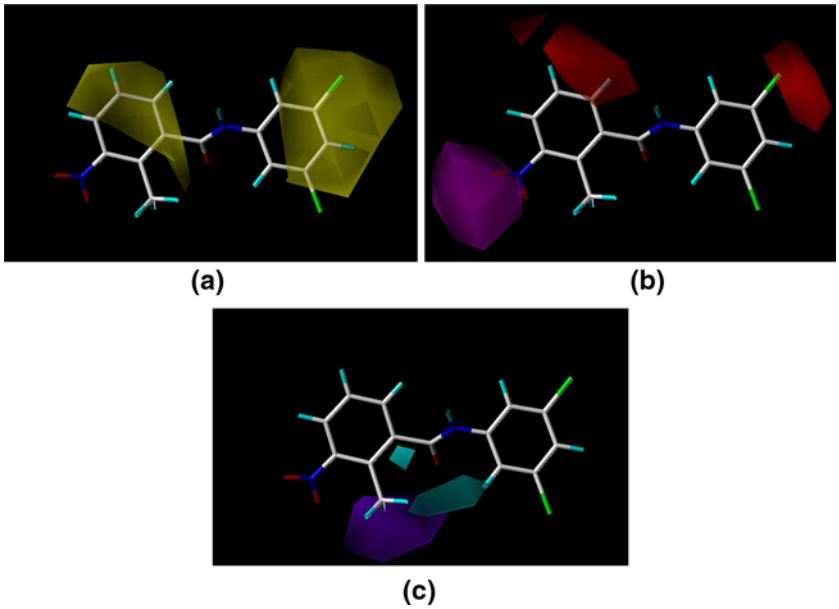

Fig. 6 CoMSIA contour maps **a** hydrophobic contours—favoured (*yellow*); **b** H-acceptor contours—favoured (*magenta*), disfavoured (*red*); **c** H-donor contours—favoured (*cyan*), disfavoured (*purple*) (Color figure online)

where for one exception—the *meta*-region of ring A, the entire ring is surrounded with yellow hydrophobic contours. Similarly, hydrophobic substitutions are suggested near the *meta*- and *para*-regions of ring B. The H-bond acceptor contours (Fig. 6b) reveal that H-bonding would be favourable if such groups are placed at the *meta*-position of ring A. The H-bond acceptor groups would diminish activity if positioned at the *ortho*- and *para*-positions of ring A and the meta- and *para*-regions of ring B. H-bond donor contours (Fig. 6c) are seen around the *ortho*-position on ring B, while the *ortho*-region of ring A disfavours H-bond donors.

With these five CoMFA and CoMSIA models, the activities of the newly designed molecules were predicted (Table 5). It can be seen in Table 3, that the r^2_{pred} for the CoMFA model is unsatisfactory; the CoMSIA models have much better predictive power for the external test set. The statistics quoted in Table 3 also reveal that except for the *F* values all other parameters are close to ideal values. In summary, it was decided to consider all five models instead of preferring one over the other.

Chemical synthesis

Syntheses of the *N*-phenylbenzamide analogs were carried out as described earlier (Fig. 7). The *N*-phenylbenzamide analogs were obtained easily by microwave-assisted condensation between esters of aromatic acids and aromatic amines. The overall yields obtained in this reaction were around 80–90% on an average. Physical constants and spectroscopic data of the molecules are given in Table S2 in the Supplementary material. The structure of the products was confirmed by IR, while for molecule KMC-6 as an example, ^{1}H NMR provided additional support of the structure (Table S2 in Supplementary data; Fig. 8).

Antimalarial activity

Two of the synthesized molecules, KMC-3 and KMC-15, were found to be active at 8.7 and 5.7 μM concentrations, respectively (Table 6). The corresponding values for chloroquine and artesunate, two of the well-established drugs for treatment of malaria, are 0.0087 and 0.0017 μM.

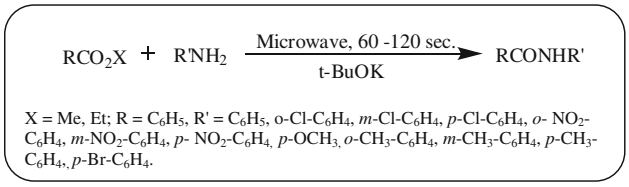

Fig. 7 General scheme for the synthesis of substituted *N*-phenylamides

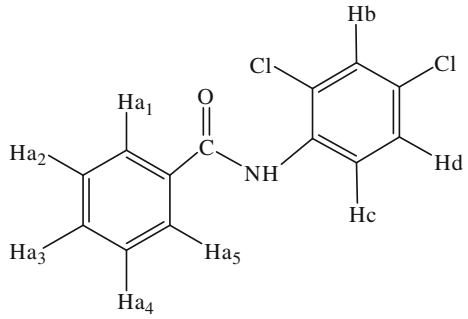

Fig. 8 Structure of *N*-(2,4-dichlorophenyl)benzamide with atom labels referred to in the discussion of ^{1}H-NMR

Table. 6 Experimental IC_{50} values of the compounds against *P. falciparum* using chloroquine and artesunate as controls

Compound ID	Experimental IC_{50} against P. *falciparum* in μM
KMC-1	>10
KMC-2	>10
KMC-3	8.7
KMC-4	>10
KMC-5	>10
KMC-6	>10
KMC-7	>10
KMC-8	>10
Chloroquine	0.087
KMC-9	>10
KMC-10	>10
KMC-11	>10
KMC-12	>10
KMC-13	>10
KMC-14	>10
KMC-15	5.7
Artesunate	0.017

In light of this, the molecules were not evaluated further as inhibitors of *P. falciparum dihydroorotate dehydrogenase*. There is thus a need for some more modifications in the structures of these molecules to improve their activity in level with chloroquine or artesunate. The CoMFA and CoMSIA models are being used in the next phase of improvement in the activity of these molecules.

Conclusions

The biosynthesis of pyrimidine nucleotides in *plasmodium* is an excellent pathway that can be targeted for the development of novel antimalarial agents. An important enzyme in this sequence of reactions is DHODH, i.e. *dihydroorotate dehydrogenase*. In the light of this, we have

focused our work on synthesis of inhibitors of DHODH as novel antimalarials. The molecules were designed with the in silico methods of docking and 3D-QSAR. Based on docking and 3D-QSAR results, we narrowed down our search to a select set of 15 substituted *N*-phenylbenzamide analogs. These molecules were synthesized in a single step using solvent-free microwave synthesis in overall yields of 80–90%; their structures were confirmed by IR and ^{1}H-NMR spectroscopy. The antimalarial activity of two of these molecules as measured by the ^{3}H-hypoxanthine method in terms of their IC_{50} values, are in the low micromolar range and modifications to their structures as suggested by the CoMFA and CoMSIA models will hopefully bring them into the nanomolar range.

Acknowledgements K. R. Desai is grateful to the All India Council for Technical Education (AICTE), New Delhi for support as JRF. The Department of Science and Technology (DST), New Delhi is thanked for facilities provided to the department through their FIST program (SR/FST/LSI-163/2003). We also would like to thank Ian Bathurst, Director, Drug Discovery and Technology, Medicines for Malaria Venture, Geneva, Switzerland and Sergio Wittlin, Head, Malaria Drug Discovery Group, Swiss Tropical Institute, Socinstrasse, Basel, Switzerland for antimalarial evaluation.

References

Baldwin J, Farajallah AM, Malmquist NA, Rathod PK, Phillips MA (2002) Malarial dihydroorotate dehydrogenase. Substrate and inhibitor specificity. J Biol Chem 277:41827. doi:10.1074/jbc.M206854200

Baldwin J, Michnoff CH, Malmquist NA, White J, Roth MG, Rathod PK, Phillips MA (2005) High-throughput screening for potent and selective inhibitors of *Plasmodium falciparum* dihydroorotate dehydrogenase. J Biol Chem 280:21847. doi:10.1074/jbc.M501100200

Baumann P, Mandl-Weber S, Volkl A, Adam C, Bumeder I, Oduncu F, Schmidmaier R (2009) Dihydroorotate dehydrogenase inhibitor A771726 (leflunomide) induces apoptosis and diminishes proliferation of multiple myeloma cells. Mol Cancer Ther 8:366. doi:10.1158/1535-7163.MCT-08-0664

Becker K, Kirk K (2004) Of malaria, metabolism and membrane transport. TRENDS Parasitol 20:590. doi:10.1016/j.pt.2004.09.004

Boa AN, Canavan SP, Hirst PR, Ramsey C, Stead AM, McConkey GA (2005) Synthesis of brequinar analogue inhibitors of malaria parasite dihydroorotate dehydrogenase. Bioorg Med Chem 13:1945. doi:10.1016/j.bmc.2005.01.017

Breman JG (2001) The ears of the hippopotamus: manifestations, determinants, and estimates of the malaria burden. Am J Trop Med Hyg 64:1

Bush BL, Nachbar RB Jr (1993) Sample-distance partial least squares: PLS optimized for many variables, with application to CoMFA. J Comput Aided Mol Des 7:587

Chiang PK, Bujnicki JM, Su X, Lanar DE (2006) Malaria: therapy, genes and vaccines. Curr Mol Med 6:309

Cramer RD, Patterson DE, Bunce JD (1988) Comparative molecular field analysis (CoMFA). 1. Effect of shape on binding of steroids to carrier proteins. J Am Chem Soc 110:5959. doi:10.1021/ja00226a005

Cramer RD III, Patterson DE, Bunce JD (1989) Recent advances in comparative molecular field analysis (CoMFA). Prog Clin Biol Res 291:161

Davis JP, Cain GA, Pitts WJ, Magolda RL, Copeland RA (1996) The immunosuppressive metabolite of leflunomide is a potent inhibitor of human dihydroorotate dehydrogenase. Biochemistry 35:1270. doi:10.1021/bi952168g

Elkayam O, Yaron I, Shirazi I, Judovitch R, Caspi D, Yaron M (2003) Active leflunomide metabolite inhibits interleukin 1beta, tumour necrosis factor alpha, nitric oxide, and metalloproteinase-3 production in activated human synovial tissue cultures. Ann Rheum Dis 62:440

Fidock DA, Rosenthal PJ, Croft SL, Brun R, Nwaka S (2004) Antimalarial drug discovery: efficacy models for compound screening. Nat Rev Drug Discov 3:509. doi:10.1038/nrd1416

Freundlich JS, Yu M, Lucumi E, Kuo M, Tsai HC, Valderramos JC, Karagyozov L, Jacobs WR Jr, Schiehser GA, Fidock DA, Jacobus DP, Sacchettini JC (2006) Synthesis and biological activity of diaryl ether inhibitors of malarial enoyl acyl carrier protein reductase. Part 2: 2′-substituted triclosan derivatives. Bioorg Med Chem Lett 16:2163. doi:10.1016/j.bmcl.2006.01.051

Gramatica P (2007) Principles of QSAR models validation: internal and external. QSAR Comb Sci 26:694

Gujjar R, Marwaha A, El Mazouni F, White J, White KL, Creason S, Shackleford DM, Baldwin J, Charman WN, Buckner FS, Charman S, Rathod PK, Phillips MA (2009) Identification of a metabolically stable triazolopyrimidine-based dihydroorotate dehydrogenase inhibitor with antimalarial activity in mice. J Med Chem 52:1864. doi:10.1021/jm801343r

Hamilton LC, Vojnovic I, Warner TD (1999) A771726, the active metabolite of leflunomide, directly inhibits the activity of cyclooxygenase-2 in vitro and in vivo in a substrate-sensitive manner. Br J Pharmacol 127:1589. doi:10.1038/sj.bjp.0702708

Heikkila T, Thirumalairajan S, Davies M, Parsons MR, McConkey AG, Fishwick CW, Johnson AP (2006) The first de novo designed inhibitors of *Plasmodium falciparum* dihydroorotate dehydrogenase. Bioorg Med Chem Lett 16:88. doi:10.1016/j.bmcl.2005.09.045

Heikkila T, Ramsey C, Davies M, Galtier C, Stead AM, Johnson AP, Fishwick CW, Boa AN, McConkey GA (2007) Design and synthesis of potent inhibitors of the malaria parasite dihydroorotate dehydrogenase. J Med Chem 50:186. doi:10.1021/jm060687j

Hurt DE, Widom J, Clardy J (2006) Structure of *Plasmodium falciparum* dihydroorotate dehydrogenase with a bound inhibitor. Acta Crystallogr D 62:312. doi:10.1107/S0907444905042642

Kalra BS, Chawla S, Gupta P, Valecha N (2006) Screening of antimalarial drugs: an overview. Indian J Pharmacol 38:5

Klebe G (1998) Comparative molecular similarity indices analysis: CoMSIA. Perspect Drug Discov Des 12:87. doi:10.1023/A:1017025803403

Klebe G, Abraham U, Mietzner T (1994) Molecular similarity indices in a comparative analysis (CoMSIA) of drug molecules to correlate and predict their biological activity. J Med Chem 37:4130

Kobayashi Y, Ueyama S, Arai Y, Yoshida Y, Kaneda T, Sato T, Shin K, Kumegawa M, Hakeda Y (2004) The active metabolite of leflunomide, A771726, inhibits both the generation of and the bone-resorbing activity of osteoclasts by acting directly on cells of the osteoclast lineage. J Bone Miner Metab 22:318. doi:10.1007/s00774-003-0489-4

Li WD, Lin ZB (2002) Effects of leflunomide and its active metabolite on the production and mRNA expression of TNF-alpha in peritoneal macrophages and synovial cells with adjuvant arthritis in rats. Yao Xue Xue Bao 37:767

McRobert L, McConkey GA (2002) RNA interference (RNAi) inhibits growth of Plasmodium falciparum. Mol Biochem Parasitol 119:273. doi:S0166685101004297[pii]

Otsuka T, Koyama T, Ohtani R, Niiro H, Yoshizawa S, Harada M, Inokuma S (2008) Leflunomide-induced lung injury that developed after its withdrawal, coinciding with peripheral blood lymphocyte count decrease. Mod Rheumatol 18:96. doi:10.1007/s10165-007-0014-z

Perreux L, Loupy A, Delmotte M (2003) Microwave effects in solvent-free esters aminolysis. Tetrahedron 59:2185. doi:10.1016/S0040-4020(03)00151-0

Phillips MA, Gujjar R, Malmquist NA, White J, El Mazouni F, Baldwin J, Rathod PK (2008) Triazolopyrimidine-based dihydroorotate dehydrogenase inhibitors with potent and selective activity against the malaria parasite *Plasmodium falciparum*. J Med Chem 51:3649. doi:10.1021/jm8001026

Quashie NB, de Koning HP, Ranford-Cartwright LC (2006) An improved and highly sensitive microfluorimetric method for assessing susceptibility of *Plasmodium falciparum* to antimalarial drugs in vitro. Malar J 5:95. doi:10.1186/1475-2875-5-95

Richard D, Cramer RD III, Bunce JD, Patterson DE, Frank IE (1988) Crossvalidation, bootstrapping, and partial least squares compared with multiple regression in conventional QSAR studies. Quant. Struct. Act. Relat. 7:18

Ridley RG (2002) Medical need, scientific opportunity and the drive for antimalarial drugs. Nature 415:686. doi:10.1038/415686a

Shao J (1996) Bootstrap model selection. J Am Stat Assoc 91:655

Wold S, Johansson E, Cocchi M (1993) In: Kubinyi H (ed) 3D QSAR in drug design: theory, methods and applications. ESCOM Science Publishers, Leiden, p 523

Yao HW, Li J, Chen JQ, Xu SY (2004a) A 771726, the active metabolite of leflunomide, inhibits TNF-alpha and IL-1 from Kupffer cells. Inflammation 28:97

Yao HW, Li J, Chen JQ, Xu SY (2004b) The active metabolite of leflunomide A771726 inhibits proliferation and collagen synthesis of hepatic stellate cell. Zhejiang Xue Xue Bao Yi Xue Ban 33:515

Zhang X, Zhou H, Dong GF, Shi YZ (2005) An exploratory study on in vitro effects and mechanism of leflunomide on dendritic cells of systemic lupus erythematosus. Zhonghua Nei Ke Za Zhi 44:370

Zhang M, Hao N, Bian F (2008) The active metabolite of leflunomide A771726 inhibits corneal neovascularization. J Huazhong Univ Sci Technol Med Sci 28:364. doi:10.1007/s11596-008-0332-1